Initial stages in the oxidation and reduction of the 4×4 surface oxide phase on Ag{111}: A combined density-functional theory and STM simulation study

M.-L. Bocquet,[1] A. Michaelides,[2] P. Sautet,[1] and D. A. King[2]
[1]*Laboratoire de Chimie, UMR 5532, Ecole Normale Supérieure, Lyon, France*
[2]*Department of Chemistry, University of Cambridge, Lensfield Road, Cambridge, CB2 1EW, United Kingdom*
(Received 7 February 2003; published 22 August 2003)

With density-functional theory, we have examined the initial stages in the oxidation and reduction of the high coverage $Ag_{1.83}O$ oxide phase that forms on Ag{111}. Various oxidized and reduced structures have been identified and their relative energies assessed at 0 K and at finite temperatures and pressures. We find that in the temperature and pressure regime characteristic of industrial epoxidation conditions, the $Ag_{1.83}O$ oxide is easily oxidized and reduced demonstrating a high chemical flexibility of this oxide for redox reactions. In addition scanning tunneling microscopy (STM) image simulations have been performed. These reveal that as well as the $Ag_{1.83}O$ oxide structure previously proposed a second oxide overlayer is consistent with reported STM images of this system, making this different oxide overlayer another likely candidate for the surface structure obtained in the experiment.

DOI: 10.1103/PhysRevB.68.075413 PACS number(s): 81.65.Mq, 82.65.+r, 68.37.Ef, 68.35.−p

I. INTRODUCTION

Silver is a unique catalyst for the selective oxidation of ethene to ethene epoxide. On moderately high exposures of oxygen or other oxidants to Ag{111}, a thin oxide overlayer forms. This oxide overlayer is thought to be key to silver oxidation catalysis and thus the nature of this reconstruction, which is characterized by a $p(4\times4)$ low-energy electron diffraction (LEED) pattern,[1] has been the subject of investigation for nearly thirty years. Through a combined scanning tunneling microscopy (STM) experiment and simulation study King and co-workers were recently able to propose a structural model for this system. It was suggested that it consists of a nonstoichiometric $Ag_{1.83}O$ oxide trilayer epitaxed to Ag{111}.[2,3] Subsequent density-functional theory (DFT) calculations lent support to the proposed structure and through the application of thermodynamic models to account for finite-temperature and -pressure effects it was suggested that this catalyst remains stable at industrial epoxidation conditions and is thus a likely candidate for the active epoxidation catalyst.[4]

However, our previous study concentrated on comparing the stability of $Ag_{1.83}O$ (or equivalently labeled $Ag_{11}O_6$) to a stoichiometric Ag_2O oxide overlayer and also to chemisorbed O adatoms. The question of the absolute stability of the $Ag_{1.83}O$ oxide as a function of small variations of O coverage remains unanswered. The question of the relative stabilities of O rich and O deficient oxide overlayers is important because the ease with which the oxide can lose and accept oxygen is of crucial significance to its activity as an oxidation catalyst.[5,6] Here we investigate this issue, primarily with DFT, by determining structures and energies for the initial stages in the oxidation and reduction of this important oxide overlayer. By applying simple thermodynamic models in conjunction with sophisticated STM image simulations to our DFT derived structures we also aim at improving the atomic level understanding of the Ag oxide overlayer at finite temperatures and pressures. We now briefly describe the theoretical approaches employed. Following this we present DFT results for the various O deficient and O rich oxide overlayers identified. STM image simulations are then presented for each oxide overlayer and finally we assess their relative stabilities at finite temperatures and pressures.

II. THEORETICAL METHODS

Density-functional calculations were performed within the plane-wave pseudopotential formalism, as implemented in the VASP code.[7] This code utilizes ultrasoft pseudopotentials and the Perdew Wang 1991 (''PW 91'') generalized gradient approximation.[8] The supercell approach is used to model the Ag oxide terminated Ag{111} surface. Each repeat unit contains a slab of three Ag{111} layers on which various Ag oxide trilayers and O atoms are adsorbed. A vacuum region of >14 Å is used to separate adjacent slabs. During all structure optimizations the bottom two layers of Ag{111} were held fixed while all other atoms were allowed to relax. For consistency with the observed experimental periodicity, a $p(4\times4)$ unit cell is always used throughout. All energies reported have been obtained with **k**-point sampling equivalent to 64 symmetric points in the Brillouin zone of a (1×1) cell. However, because of the large size of the calculations, with >500 electrons treated explicitly, the 64 symmetric points were used merely to obtain energies based on structure optimizations performed with reduced **k**-point sampling equivalent to 16 symmetric points.

The temperature and pressure dependence on the stability of the various O rich and O deficient overlayers was compared through their Gibbs' free energies of adsorption. The Gibbs free energy of adsorption[9] (ΔG) is

$$\Delta G(T,P)=[G(\mathrm{O/Ag\{111\}})-G(\mathrm{Ag\{111\}})-11\mu_{\mathrm{Ag}}(T,P)-N_{\mathrm{O}}\mu_{\mathrm{O}}(T,P)]. \quad (1)$$

Here G(O/Ag{111}) denotes the total Gibbs free energy of our oxide covered Ag surfaces. G(Ag{111}) is the total Gibbs free energy of the clean three layer Ag{111} slab. μ_{Ag} is the

chemical potential of the (11) excess Ag atoms that are present in the oxide overlayer. This is simply our DFT computed total energy of a bulk Ag atom. μ_O is the chemical potential of O and N_O is the number of O atoms in the super cell. The chemical potential of O is referenced to oxygen molecules in the gas phase for which we use the ideal gas equation. It is well known that the ideal gas equation suffers deficiencies at low temperatures and high pressures. Fortunately under the conditions we are primarily interested in (high temperatures and moderate pressures) it is a well-behaved approximation. With this approach we investigate the temperature and pressure dependence of μ_O and thus the temperature and pressure influence on the stability of the various oxide phases. However, in the present study, as before,[4] we have neglected pressure, vibrational, and configurational effects on the Gibbs free energy of our solid slabs, i.e., the Gibbs free energy appearing in Eq. (1) is approximated by the total energy at zero temperature. This is justified since variations in these terms with temperature and pressure tend to be overwhelmed by the corresponding variations of the gas phase molecules (which we include explicitly).[10,11] Moreover, this omission is further mitigated since we are concerned with assessing the relative stabilities of adsorbed overlayers, and thus what is actually neglected is differences in these contributions. Nonetheless, in the following, we are careful not to make any conclusions based on small energy differences between the models tested, which would not be justified in the present study.

The STM image simulations performed on our optimized DFT structures utilize a Green's-function based elastic scattering formalism and take into account the entire quantum chemical interaction between the surface and the tip. The formalism behind these simulations has been described in detail elsewhere.[12] The key feature of this approach is that it provides an atom by atom description of the entire STM interface allowing various tip structures. For all the simulated images presented here the tip is modeled as an isolated rigid pyramid of W atoms stacked on top of a W{110} surface. The electronic structures used in the STM simulations are approximated using an effective Hückel-type Hamiltonian which has been parametrized[13] based on DFT density of states (DOS) plots.

III. INVESTIGATION OF THE REDUCED AND OXIDIZED Ag_xO OXIDE OVERLAYERS

Figures 1(a) and (b) illustrate the previously determined structural model for the $Ag_{1.83}O$ oxide trilayer epitaxed to Ag{111}. This is the reference oxide overlayer and it consists of hexagonal Ag-O-Ag rings, with a coverage of 0.375 monolayer (ML) of oxygen. It has a $p(4\times4)$ periodicity [indicated by the black dotted line parallelogram in Fig. 1(a)] with three Ag-O-Ag rings per (4×4) unit cell. In a single unit cell, two of the oxide rings contain an additional chemisorbed Ag adatom whilst in the third [center of the unit cell in Fig. 1(a)] there is no such Ag adatom. Throughout the paper we shall call the oxide rings that contain Ag adatoms ''filled'' rings and the oxide rings that do not contain additional Ag adatoms ''vacant'' rings. One important feature to recognize in this complex overlayer is the location of these additional chemisorbed Ag atoms since they are selectively imaged by the STM and produce the characteristic hexagonal images. The STM resolved hexagonal arrangement of the Ag adatoms is recalled by bold black circles around them in Fig. 1(b). In order to simulate oxidation and reduction of this reference silver oxide overlayer, O atoms were either added to it or removed from it.

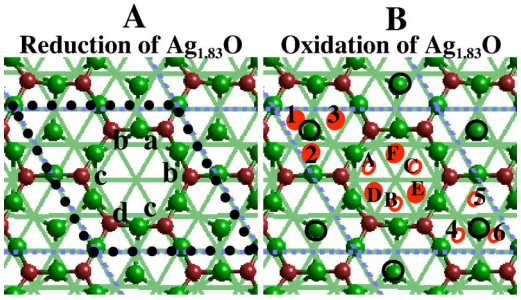

FIG. 1. Plan views of the structure of the $Ag_{1.83}O$ (or $Ag_{11}O_6$) oxide layer on Ag{111}. The central $p(4\times4)$ unit cell is indicated by the black bold dotted parallelogram (side A). Green sticks represent the Ag substrate. Green (dark red) balls depict Ag (O) atoms in the oxide overlayer. In side A, removable oxygens atoms are marked with labels a–d. In side B, full (empty) red circles mark the possible hcp (fcp) sites for additional oxygen atoms that simulate a step by step oxidation process. Labels A–E designate threefold sites in the vacant oxide ring of the unit cell, while numbers 1–6 are given for threefold sites in the vicinity of Ag adatom inside the filled oxide ring. In side B, an additional black circle surrounds Ag adatoms that produce the characteristic STM honeycomb image.

A. $Ag_{2.2}O$ oxide overlayer

First we shall consider the initial stages in the reduction of our reference $Ag_{1.83}O$ oxide overlayer. In order to model the reduction process, several structures with one ($Ag_{2.2}O$) and then two ($Ag_{2.75}O$) oxygen atoms removed have been tested. First, a single O atom was removed from the oxide overlayer. In any Ag-O-Ag oxide ring there are three higher-lying and three lower-lying O atoms. We find that, within the accuracy of our calculations, it costs the same energy ($\sim$0.8 eV to yield $1/2O_2$[10]) to remove a higher-lying O [for example, O*a* in Fig. 1(a)] as it does to abstract a lower-lying O [for example, Ob in Fig. 1(a)] from the $Ag_{11}O_6$ oxide overlayer. The resulting optimized structure obtained when a higher-lying O (O*a*) is removed is shown in Fig. 2. It can be seen that once a single O is removed from the reference oxide the three Ag atoms of the oxide overlayer, which had previously surrounded the extracted O, move to produce a triangle of chemisorbed Ag atoms. Hence on the surface, the cleavage of Ag-O bonds is compensated by the strengthening of Ag-Ag bonds and represents a transition from a local oxide to a local metallic environment.

B. $Ag_{2.75}O$ oxide overlayer

Following the removal of the first O, a second O was then removed from the Ag oxide overlayer to produce an oxide with a stoichiometry of $Ag_{2.75}O$. Specifically, systems with

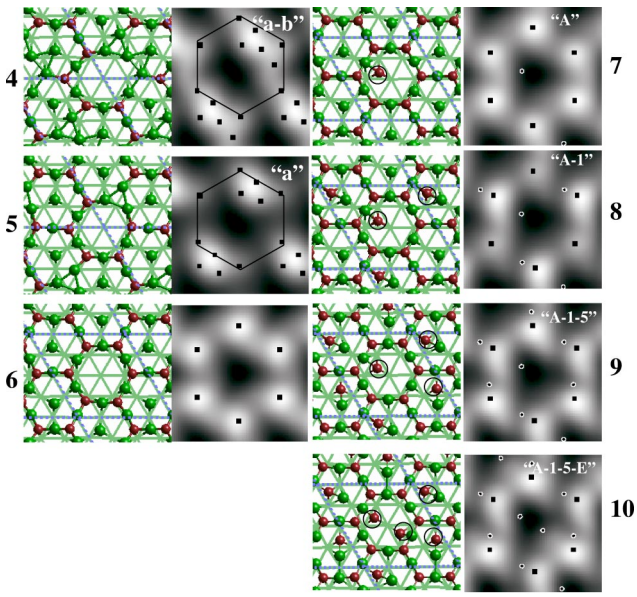

FIG. 2. Plan view structures (left side) and associated STM simulations (right side) for the most stable configurations when increasing the number of surface oxygen atoms per $p(4\times4)$ unit cell from 4 to 10 oxygen atoms. The reference $Ag_{1.83}O$ oxide contains six O atoms per $p(4\times4)$ unit cell. Left side: Each structure shows the successive addition of a single oxygen corresponding to coverage ratio going from 0.25, 0.31, 0.37, 0.43, 0.5, 0.56, to 0.62 ML, respectively. Black circles surround the location of extra atomic oxygens compared to the structure of the reference oxide. Labels (letter or/and numbers) defined in Fig. 1 for defining the position of extra atoms are reported for the sake of clarity. Right side: Plan views of the STM current simulations of each oxide structure. The tunneling parameters are similar to the reported experimental values ($V=100$ mV, W tip) in order to get current of nA magnitude. The image current corrugations are 10.7, 13, 5.2, 5.7, 8.9, 9.8, and 10.8 nA, respectively from the oxide containing four oxygen atoms ($Ag_{2.75}O$) to the one containing ten oxygen atoms ($Ag_{1.1}O$). Black squares mark the position of metallic Ag atoms (not directly linked to an oxygen). In the reduced structures ($Ag_{2.2}O$, $Ag_{2.75}O$) the honeycomb trace is reproduced. Small white rings mark the position of extra oxygens.

O atoms labeled (a) and (b), (a) and (c), and (a) and (d) removed were examined [Fig. 1(a)]. It is found that the most stable of these three doubly reduced oxide systems is the arrangement in which the O atoms labeled (a) and (b) are removed. It costs ~1 eV to remove (b) after (a) is removed. And there is a ~0.2-eV preference to remove the pair of O atoms (a)–(b) over the two other possibilities [(a)–(c) and (a)–(d)], which show essentially the same stability. This reveals that there is a greater tendency to remove a pair of O atoms that are adjacent to each other as opposed to any pair of O atoms that are next-nearest neighbors or even further apart. The structure of the most stable doubly reduced $Ag_{2.75}O$ oxide overlayer [(a)–(b) removed] is displayed in Fig. 2. This structure is very interesting and it reveals that two Ag triangles matching the underlying Ag{111} have been formed. Indeed these triangular structures appear every time an O is removed and resemble, albeit on a much smaller scale, the islands observed by STM that form upon oxide decomposition. The formation of a single ''metallic'' island by the removal of two adjacent O atoms is favored over the formation of two separated Ag3 triangles, because it allows an easier relaxation of these Ag atoms, with less induced surface strain upon local reduction.

C. $Ag_{1.57}O$ oxide overlayer

Oxidation of the reference $Ag_{1.83}O$ oxide was examined by adding chemisorbed O atoms to the system. Chemisorbed O atoms were added to threefold hollow sites, which are known to be the most stable adsorption sites for O on Ag{111}.[4,14] However, given the complexity of the (4×4) oxide overlayer there are a total of 12 threefold adsorption sites in the unit cell. These are shown in Fig. 1(b) with fcc and hcp sites distinguished by empty and filled circles, respectively. There are three fcc and three hcp sites [indicated by the capital letters in Fig. 1(b)] inside the vacant oxide ring. There are three further hcp sites inside one of the filled oxide rings (labeled 1–3) and a further three fcc sites inside the second filled oxide ring (labeled 4–6). It should not be overlooked, however, that the six threefold sites in the two filled oxide rings are all in the vicinity of chemisorbed Ag adatoms and are thus not strictly threefold symmetric.

Addition of the first oxygen atom was considered at four representative and nonequivalent adsorption sites: an fcc (site A) and an hcp (site E) site inside a vacant oxide ring, and an fcc (site 5) and an hcp (site 3) site inside a filled ring. It is found that O binds with a similar energy, to within ~0.1 eV, at all four adsorption sites and decreases on going from $5>A>3>E$. This indicates that small preferences exist for adsorption at fcc sites over hcp sites and in filled rings over vacant rings. The energetic differences between fcc and hcp are 0.05 and 0.1 eV in filled and vacant rings, respectively, and obey the classic rules for the O/Ag{111} adsorption system.[4] Thus we conclude that addition of the first oxygen atom is not selective thermodynamically and it does not have any strong energetic preference for adsorption in filled over vacant oxide rings. Adsorption in filled oxide rings is, however, accompanied by a large displacement of the chemisorbed Ag adatom. It is plausible therefore that adsorption in the ''vacant'' rings (site A for example), where no such reconstruction is required may be kinetically favored. Indeed, the inclusion of a chemisorbed O atom inside a vacant oxide ring has a negligible effect on the structure of the initial $Ag_{1.83}O$ oxide, as can be seen in Fig. 2. The O adsorption energy at site A is -0.5 eV again with respect to the formation of 1/2 O_2.[15] We find that, using an identical level of theory, this is 0.2 eV less than the O adsorption energy on clean Ag{111}. A consideration of the structure reveals that this is likely because the chemisorbed O is bonding with a surface Ag atom that is already interacting to lower oxygens in the oxide overlayer.

D. $Ag_{1.37}O$ oxide overlayer

For the adsorption of two oxygen atoms on the reference $Ag_{1.83}O$ oxide, a number of combinations mixing the 12 threefold sites are possible. Several possibilities have been considered. Let us consider them. First we considered adding

two oxygens to the same oxide ring. By placing an O atom at site A and a second O at site E, we find, however, that there is a strong repulsion between the O atoms. For example, the binding energy of O at site E in the presence of an O at site A is $\sim +0.3$ eV (relative to $1/2O_2$ in the gas phase[10]). Since the O adsorption properties inside vacant and filled rings are similar it is anticipated that an equally large repulsion will characterize the adsorption of two O atoms in the filled oxide rings. Strong repulsion between O atoms adsorbed in the same oxide rings is important because it establishes that if a second O is to be added to the unit cell then it is more likely to adsorb in a different oxide ring to the first O.

If we consider arrangements of the two extra oxygens with these oxygens inside different oxide rings we find that either both oxygens can adsorb in two filled oxide rings, or one can adsorb in a vacant ring and the other in a filled ring. Because of the periodic boundary conditions with a single O atom in each of the two filled oxide rings these oxygen atoms are occupying threefold sites which share a Ag atom, or which are further separated. For example, the former case may correspond to the occupation of sites 1 and 6 and a direct O-O distance of 2/sqrt(3) the Ag-Ag distance. The latter case with co-adsorption on sites 3 and 5, for example, corresponds to twice the previous closest distance. We find that the latter arrangement with O atoms at completely distinct threefold sites (sites 3 and 5) is preferred energetically by 0.3 eV.

For the alternative situation when we have one O in a vacant ring and one O in a filled ring we have considered several trial structures. Specifically the following arrangements of O atoms were considered: A-3, A-4, A-6, A-1. Although they have not been examined, the arrangements A-2 and A-5 are essentially equivalent to A-3 and A-4. Of the many arrangements considered (and listed above) for the adsorption of two O atoms on the reference $Ag_{1.83}O$ oxide we find that the most stable configuration is to have the O atoms at site A and site 1. The structure of this overlayer is shown in Fig. 2. The average adsorption energy for these two additional O atoms is ~ -0.5 eV. The stability of the various arrangements decreases in the order: A-1>3-5>A-5 >A-3>A-6. Aside from the arrangement A-6, which is highly destabilized compared to the others, this trend is correlated with a decrease in the nearest distance between the pair of chemisorbed O atoms. For the A-6 situation from Fig. 1(b), it can be guessed that filling positions 6 of adjacent cells implies two identical nearest distances (twice the Ag-Ag distance) instead of one for all other cases. This induces an effective trimer of O atoms instead of a dimer.

E. $Ag_{1.22}O$ oxide overlayer

Three O adatoms were then added to the oxide overlayer to produce an $Ag_{1.22}O$ overlayer. Since we know that two O atoms do not like to adsorb in the same oxide ring adding a third oxygen supposes that all three oxide rings per unit cell contain a single additional chemisorbed O atom. Three alternative arrangements of the three chemisorbed O atoms were considered. In these, O atoms were either at: (i) sites A,1 and 5; (ii) A,3 and 5; and (iii) A,1 and 6. We find that the arrangement A-1-5 (Fig. 2) is clearly favored again with a average binding energy of the three O atoms of -0.5 eV.

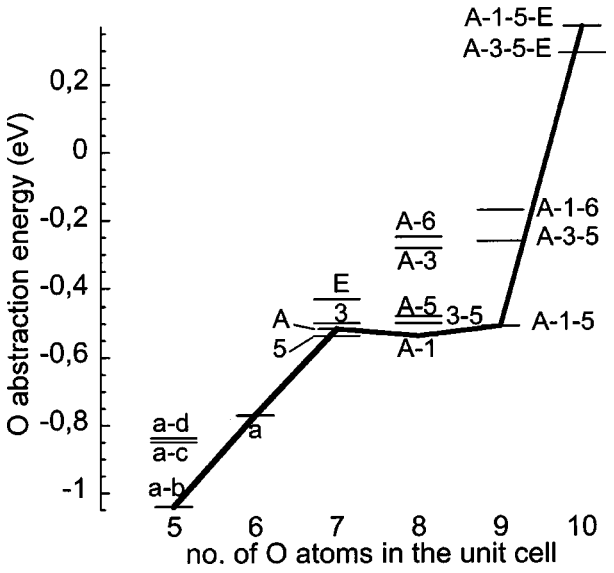

FIG. 3. Oxygen abstraction energy, starting from five to ten oxygen atoms in the oxide overlayer. Labels (letter+numbers) are those defined in Fig. 1 to position extra or removed oxygen atoms. A straight line links the most favorable connected configurations and defines a possible scenario for a step by step oxidation process.

F. $Ag_{1.1}O$ oxide overlayer

Further oxidation of the $Ag_{1.83}O$ oxide overlayer, i.e., addition of a fourth O atom to the unit cell, has lastly been examined. Since there are three oxide rings per unit cell adding four oxygens almost certainly requires that at least two O atoms must be added to at least one of the oxide rings. Although it was established above that two O atoms do not like to adsorb in the same oxide ring for completeness two structures with ten O atoms per cell ($Ag_{1.1}O$) were examined. These had O atoms at sites A,3,5 and E, and A,1,5 and E. However, as anticipated both of these structures become highly unstable ($+0.3$ eV and $+0.4$ eV for the tenth O binding energy, respectively) with the average adsorption energy of the four additional chemisorbed O atoms now weakened to -0.3 eV. This result is important because it indicates that with the addition of three additional chemisorbed O atoms, equivalent to the addition of 0.19 ML O atoms, the $Ag_{1.83}O$ oxide overlayer becomes saturated to the addition of chemisorbed O atoms. Obviously it is always possible that further oxidation takes place by some other mechanism, for example oxide growth facilitated by penetration of O atoms into the bulk.[16] However, alternative mechanisms for oxidation are beyond the scope of the present study and have not been investigated yet.

The relative energetics of all the investigated oxidized and reduced structures from the above sections are summarized in Fig. 3 with their associated labels as defined in Fig. 1(b). Specifically in Fig. 3 the ''O abstraction energy'' of certain O atoms in all the overlayers investigated are represented and compared. The O abstraction energy is the energy required

to remove a given O atom from an oxide overlayer of a given stoichiometry to form 1/2 O_2. We define this energy as: $E^{O}_{abstr}(n) = (Ag_{11}O_n/Ag) - (Ag_{11}O_{(n-1)}/Ag) - 1/2O_{2\,(g)}$; $Ag_{11}O_n/Ag$ is the computed total energy of the given oxide, $Ag_{11}O_{(n-1)}/Ag$ the total energy of the most stable associated reduced oxide, and $O_{2(g)}$ the total energy of the gas phase O_2 molecule. For example, Fig. 3 indicates that the energy required to remove O*a* from the $Ag_{1.83}O$ overlayer (six oxygens per cell) is ~ 0.8 eV. It is clear that the oxygen abstraction energy reaches a plateau around -0.5 eV for the successive filling of available oxide rings starting from the reference oxide. This is consistent with an energetic equivalence of the O adsorption energy inside all three oxide rings in a cell. Further, the abstraction energy of the tenth O in the cell is positive, again demonstrating the onset of saturation of the $Ag_{1.83}O$ oxide overlayer at the point when all three rings contain a chemisorbed O atom ($Ag_{1.22}O$). As stressed above this strong repulsion is attributed to the fact that in this configuration the chemisorbed oxygen atoms must share bonding with the same Ag substrate atom. The solid line in Fig. 3 marks a possible sequential atomic mechanism when oxidizing a reduced $Ag_{2.75}O$ structure.

IV. STM SIMULATIONS

Having determined structures for possible reduced and oxidized Ag oxide overlayers on Ag{111} we then performed STM image simulations on the most stable structure at each stoichiometry. The results of the simulations are shown in Fig. 2 alongside the structure of each oxide overlayer. The key finding is that a second Ag oxide overlayer, in addition to the reference $Ag_{1.83}O$ oxide, is identified that exhibits the same characteristic honeycomb image observed experimentally.[2] This is the $Ag_{1.83}O$ oxide with a single additional O adsorbed inside each vacant Ag-O-Ag ring (i.e., $Ag_{1.57}O$ with O at site A). In fact the simulated images for the $Ag_{1.83}O$ and $Ag_{1.57}O$ oxide systems are essentially indistinguishable. This is clearly related to the fact that the Ag adatoms in the filled rings, which are responsible for the STM contrast are not significantly perturbated by the additional O adsorbate.

It is also seen from Fig. 2, however, that *all* the images associated with oxygen rich oxide overlayers ($Ag_{1.37}O$ to $Ag_{1.1}O$) are reasonably similar to the reference honeycomb image ($Ag_{1.8}O$ and $Ag_{1.57}O$). The image associated with $Ag_{1.37}O$ (''A-1'') exhibits a reduced threefold symmetry since half the metallic Ag adatoms are displaced outward by the presence of the extra oxygen atoms. Equivalent maximum current values are recovered for $Ag_{1.2}O$ (''A-1-5'') where all the Ag adatoms are now affected. The image is, however, slightly distorted with respect to the reference $Ag_{1.83}O$ case. As would be expected there is no visible difference between the image $Ag_{1.2}O$ and $Ag_{1.1}O$ since the only difference in their structures is the presence of a single O in the dark region of STM contrast. On the other hand, both configurations associated with the O deficient oxide overlayers exhibit significantly different images associated with the creation of new metallic Ag atoms at the surface. The current maxima are clearly related with the metallic Ag_3 triangles

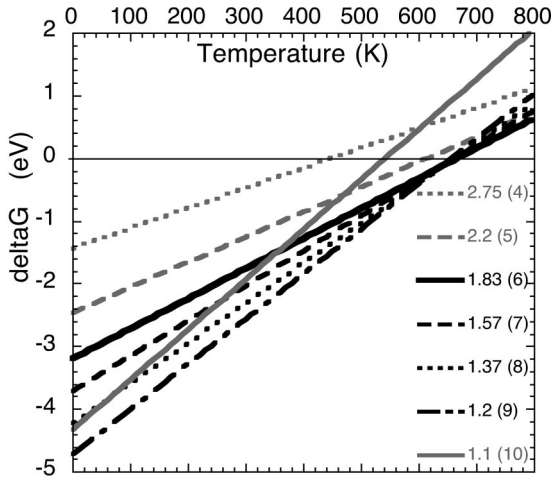

FIG. 4. Gibbs energy of adsorption (ΔG) against temperature at 15 atm of oxygen (industrial reaction pressure) for the most stable oxide overlayer at each stoichiometry, as shown in Fig. 2. The legend gives the stoichiometry of the oxide surface, with the number of oxygen in a $p(4\times4)$ unit cell between parentheses.

formed upon reduction. In particular the sixfold symmetry of the contrast is lost.

To conclude, the simulations indicate that it should not be possible for the STM to distinguish between the $Ag_{1.8}O$ oxide and a singly oxidized version of it ($Ag_{1.57}O$). Or put another way, O adatoms adsorbed inside the vacant Ag oxide rings should be invisible to the STM. Given that the simulated STM images for structures with more O adatoms are also reasonably similar it is plausible that the Ag oxide overlayer that forms on Ag{111} could well be $Ag_{1.83}O$ or one of the higher coverage oxide overlayers. Indeed the higher coverage oxides display O coverages of 0.43 ML ($Ag_{1.57}O$), 0.5 ML ($Ag_{1.37}O$), and 0.56 ML ($Ag_{1.2}O$), which are in closer agreement with the reported experimental range (0.45^{17}–0.51^{18} ML) for the (4×4) Ag oxide overlayer. On this basis, Raukema *et al.* already suggested the presence of excess randomly absorbed oxygen prior to oxide growth. Our DFT calculations and STM image simulations support this proposal and provide clear information on the possible location of the additional chemisorbed O adatoms.

V. EXTENSION TO INDUSTRIAL EPOXIDATION CONDITIONS

Figure 4 plots the free energy of adsorption as a function of temperature for the most stable Ag oxide overlayer at each O coverage. The pressure is 15 atmospheres which is characteristic of the pressure used in industrial epoxidation catalysis.[19] We find that at 0 K the most stable overlayer is the $Ag_{1.22}O$ overlayer, i.e., the Ag oxide with an additional O adatom inside each oxide ring (and a total of nine oxygen atoms in the unit cell). Indeed it is apparent from Fig. 4 that at 0 K the relative stability of the various oxide overlayers simply increases with the number of oxygens present up to the $Ag_{1.22}O$ oxide, after which the addition of a tenth O is unfavorable since the oxide saturates for the addition of further chemisorbed O atoms at this stage.

At this pressure and at low temperature the $Ag_{1.22}O$ oxide is most stable. As the temperature is raised, however, its stability compared to reduced structures like ($Ag_{1.83}O$, $Ag_{1.57}O$, $Ag_{1.37}O$) decreases and at 550–650 K up to four oxide overlayers ($Ag_{1.83}O$, $Ag_{1.57}O$, $Ag_{1.37}O$, and $Ag_{1.22}O$) become equally stable, with the $Ag_{1.83}O$ overlayer marginally favored as the clean surface stability curve (horizontal axis) is crossed at ~680 K. At no stage do the lower oxygen ratio oxides (modeling the reduction mechanism) become the most stable phases.

Qualitatively this scenario is the same at low pressure characteristic of the STM chamber. The effect of decreasing the pressure is simply to shift all the oxide curves to lower temperatures by around 250 K. In light of this similarity they are not shown in Fig. 4. In fact, in our previous study careful comparisons with STM experiments were made,[4] with a somewhat more accurate DFT model for the Ag substrate. We see from Fig. 4 that the relative stabilities change quite a lot as we go to higher temperatures and pressures. Precisely at reaction temperature (around 600 K) four phases (the reference system and oxidized models) become equally stable. In addition the phases with less oxygen tend to become more and more favorable at increasing temperature. It implies that it may cost less and less free energy to reduce the reference oxide at finite temperature and pressure. Oxidation or reduction processes between $Ag_{1.83}O$, $Ag_{1.57}O$, $Ag_{1.37}O$, and $Ag_{1.22}O$ proceed with almost no free-energy variation in a large range around reaction temperature. This demonstrates a remarkable flexibility of this oxidized Ag surface for redox processes. The $Ag_{1.57}O$, $Ag_{1.37}O$, and $Ag_{1.22}O$ overlayers in particular should be the best candidates for oxidation catalyst, since O abstraction can occur with no free-energy cost.

VI. CONCLUSION

The structure and energetics of several possible O deficient and O rich Ag oxide overlayers on Ag{111} have been determined. Oxidation of the reference $Ag_{1.83}O$ oxide is exothermic. Up to three chemisorbed O atoms can be added and then the oxide becomes saturated to the addition of further chemisorbed O atoms. Moreover, the chemisorbed O atoms added do not significantly modify the structure of the oxide overlayer. The only noteworthy structural changes upon the addition of O atoms are that the Ag adatoms get displaced upward when O atoms are added to the filled oxide rings. By combining DFT and STM simulation results, we find that two models match quantitatively the experimental STM images.[2] Indeed the STM simulations for $Ag_{1.83}O$ with a single additional O, i.e., $Ag_{1.57}O$ and $Ag_{1.83}O$ are virtually indistinguishable. Moreover, simply in terms of the STM simulations, up to four of the oxygen rich oxide overlayers match the experimental image reasonably well. To resolve this particular issue of whether additional O atoms are present in the Ag oxide overlayer will require a quantitative experimental analysis such as LEED.

The second aspect of this study relates to the relative stability of the various oxide layers as a function of temperature and pressure. The free-energy plots presented here go beyond standard DFT results and enable us to bridge the pressure and materials gaps and make predictions about the relative stabilities of the investigated phases in the high-pressure regime. This analysis is very illuminating and shows the true activity of the Ag catalyst at finite temperatures and pressures. From the free-energy plots we learn that at the temperatures and pressures typical of industrial epoxidation conditions surface terminations with different oxygen content have a remarquably similar stability, creating hence ideal thermodynamic conditions for redox processes. This indicates that the reference $Ag_{1.8}O$ oxide overlayer as well as some of the reduced and oxidized analogs identified here may make good oxidation catalysts, especially for the investigation of ethene oxidation mechanisms. Indeed, a theoretical study of the mechanism of ethene epoxidation has recently been performed on the $Ag_{1.8}O$ oxide overlayer.[20]

ACKNOWLEDGMENTS

M.L.B. and P.S. thank D. Loffreda for helpful discussions, J. Cerda for providing the most recent version of the STM simulation code, and IDRIS for allowing CPU time through Project 609. A.M. wishes to thank Gonville and Caius College, Cambridge, for financial support.

[1] G. Rovida, F. Pratesi, M. Maglietta, and E. Ferroni, Surf. Sci. **43**, 230 (1974).

[2] C. I. Carlisle, D. A. King, M.-L. Bocquet, J. Cerda, and P. Sautet, Phys. Rev. Lett. **84**, 3899 (2000).

[3] C. I. Carlisle, T. Fujimoto, W. S. Sim, and D. A. King, Surf. Sci. **470**, 15 (2000).

[4] A. Michaelides, M.-L. Bocquet, P. Sautet, A. Alavi, and D. A. King, Chem. Phys. Lett. **367**, 344 (2003).

[5] K. Reuter, C. Stampfl, M. V. Ganduglia-Pirovano, and M. Scheffler, Chem. Phys. Lett. **352**, 311 (2002).

[6] C. Stampfl, M. V. Ganduglia-Pirovano, K. Reuter, and M. Scheffler, Surf. Sci. **500**, 368 (2002).

[7] G. Kresse and J. Furthmüller, Comput. Mater. Sci. **6**, 15 (1996); Phys. Rev. B **54**, 11 169 (1996).

[8] J. P. Perdew, J. A. Chevary, S. H. Vosko, K. A. Jackson, M. R. Pederson, D. J. Singh, and C. Fiolhais', Phys. Rev. B **46**, 6671 (1992).

[9] The surface free energy is commonly used to account for the stability of a bulk phase as a function of temperature and pressure. Since we are concerned with oxide formation on an already prepared metal surface, we work with a relative surface free energy. This ''free energy of adsorption'' is the difference between two surface free energies (the oxide/metal and the metal). It can be viewed as an adsorption process where the adsorbate is composed of the constituent atoms of the oxide overlayer and thus includes the energy change upon taking O and Ag atoms from their respective thermodynamic reservoirs and putting them into the oxide overlayers. This term is different from the

energy of adsorption or heat of adsorption since these refer to other state functions: U and H, respectively.

[10] Throughout, the O binding energies quoted are referenced to gas phase O_2. The atomic binding energy is obtained by adding the O_2 bond strength (3.28 eV from VASP) to the values given.

[11] K. Reuter and M. Scheffler, Phys. Rev. B **65**, 035406 (2002).

[12] J. Cerda, M. A. Van Hove, P. Sautet, and M. Salmeron, Phys. Rev. B **56**, 15 885 (1997).

[13] J. Cerda and F. Soria, Phys. Rev. B **61**, 7965 (2000).

[14] W. X. Li, C. Stampfl, and M. Scheffler, Phys. Rev. B **65**, 075407 (2002).

[15] The adsorption energy (Eads) per O atom on the $Ag_{1.83}O$ oxide is calculated from: $\mathrm{Eads} = \mathrm{O} + \mathrm{Ag}_{1.83}\mathrm{O/Ag} - \mathrm{Ag}_{1.83}\mathrm{O/Ag} - 1/2\mathrm{O}_{2(g)}$; where $\mathrm{O} + \mathrm{Ag}_{1.83}\mathrm{O/Ag}$ and $\mathrm{Ag}_{1.83}\mathrm{O/Ag}$ are the total energies of the $Ag_{1.83}O$ oxide overlayer with and without the chemisorbed O atom and O_2 is the total energy of a gas phase O_2 molecule.

[16] W. X. Li, C. Stampfl, and M. Scheffler, Phys. Rev. B **67**, 045408 (2003).

[17] A. Raukema, D. A. Butler, F. M. A. Box, and A. W. Kleyn, Surf. Sci. **347**, 151 (1996).

[18] S. R. Bare, K. Griffiths, W. N. Lennard, and H. T. Tang, Surf. Sci. **342**, 185 (1995).

[19] J. M. Berty, in *Ethylene Epoxide Synthesis, Applied Industrial Catalysis*, edited by B. Leach (Academic Press, New York, 1983), Vol. 1.

[20] M.-L. Bocquet, A. Michaelides, D. Loffreda, P. Sautet, A. Alavi, and D. A. King, J. Am. Chem. Soc. **125**, 5620 (2003).